Reactive and Functional Polymers 131 (2018) 174–180

Contents lists available at ScienceDirect

Reactive and Functional Polymers

journal homepage: www.elsevier.com/locate/react

A new ITO-compatible side chain-functionalized multielectrochromic polymer for use in adaptive camouflage-like electrochromic devices

Sermet Koyuncu[a], Fatma Baycan Koyuncu[b,c,*]

[a] Department of Chemical Engineering, Faculty of Engineering, Canakkale Onsekiz Mart University, 17100, Canakkale, Turkey
[b] Department of Chemistry, Faculty of Sciences and Arts, ÇanakkaleOnsekiz Mart University, 17020 Çanakkale, Turkey
[c] Polymeric Materials Research Laboratory, Çanakkale Onsekiz Mart University, 17020 Çanakkale, Turkey

ARTICLE INFO

Keywords:
Electrochromic polymers
2,5-di-(2-thienyl)-1H-pyrrole
Adaptive camouflage

ABSTRACT

In this study, a new electroactive monomer, 3-(2-[4-(2,5-di-2-thienyl-1*H*-pyrrol-1-yl)phenyl]ethyl-thio)propanoic acid (SNSPA), was synthesized and then deposited onto the ITO/glass surface by an electrochemical process. When positive potentials were applied on the polymer film of SNSPA, the film at the neutral state turned from orange to green (0.6 V) and then to blue (1.1 V) because of the presence of polaronic and bipolaronic species on the SNS main chain of the polymer. At the last stage, a complementary electrochromic device was constructed by using poly(SNSPA) as the anode layer and PEDOT:PSS as the cathode layer. A fast response time (about 0.5 s) and a high stability of about 98% were obtained at the end of 1000 cycles. The capability of the proposed polymer to undergo reversible color change among brown, green, and blue is a significant property for use as an adaptive camouflage material for all conditions of sand, forest, and sea for military applications.

1. Introduction

With the discovery of the first conductive polymer polyacetylene by Heeger et al. [1], a new door has been opened for the technology and semi-conducting polymers with a conjugated structure; these polymers have been widely used in many areas such as light-emitting diodes [2], solar cells [3, 4], field effect transistors [5, 6], and electrochromic materials [7, 8]. Semi-conducting polymers are usually colored because of the presence of conjugated main chain; hence, the energy gap between their HOMO-LUMO levels corresponds to the energy of the visible region [9, 10]. The neutral state color of conjugated polymers is important especially for use in electrochromic materials because of the observation of reversible optical changes in absorption or permeability during electrochemical switching and the change in color [11]. Although the initial studies on electrochromic materials have started with inorganic compounds such as tungsten trioxide (WO_3) [12] and iridium dioxide (IrO_2) [13], today electroactive polymers can be widely used because of their some advantages such as structurally controllable HOMO–LUMO band gap, solution processability, high contrast ratio, and fast response time [14, 15].

Polymeric electrochromics have been extensively studied for the last 20 years; nevertheless, the materials cannot be commercialized at the desired level [16]. There are some important reasons to use these materials in commercial electrochromic applications, such as fast response time, optical density variations, percent transmittance/luminescence changes, low power requirement, high coloration efficiency (CE), and easy chemical structure modification for color adjustment [17]. Besides, the most important disadvantage of electrochromic devices (ECDs) fabricated from conducting polymers is high stability against atmospheric condition and switching voltage [18]. For this purpose, conjugated polymers functionalized with subunits such as siloxane, carboxylic acid, and phosphonic acid compatible with ITO/glass surface are good alternatives to eliminate this problem [19–21].

2,5-di-(2-thienyl)-1H-pyrrole (SNS) derivatives are very well known electroactive structure in the literature [22, 23]. Conjugated polymers containing SNS moiety are often used in electrochromic applications because of simple synthetic strategy, low oxidation potential, and reversible redox behavior [24–26]. The SNS-based polymers have different colors at the neutral state and generally converted to dark blue upon electrochemical oxidation [26]. In addition, the optical and electrochemical properties and also electrochromic performances can be easily adjusted by attaching second electroactive moiety on the side chain [27–30].

In this work, a new SNS-based electroactive polymer film containing carboxyl subunit compatible with the ITO/glass surface was prepared by electrochemical process. The AFM image shows that a well-ordered polymer film can be obtained by using potentiodynamic electrochemical polymerization onto the ITO/glass surface. Spectro-

* Corresponding author at: Department of Chemical Engineering, Faculty of Engineering, Canakkale Onsekiz Mart University, 17100 Canakkale, Turkey.
E-mail address: fatmabaycan@hotmail.com (F.B. Koyuncu).

https://doi.org/10.1016/j.reactfunctpolym.2018.07.024
Received 12 June 2018; Received in revised form 29 July 2018; Accepted 30 July 2018
Available online 31 July 2018
1381-5148/

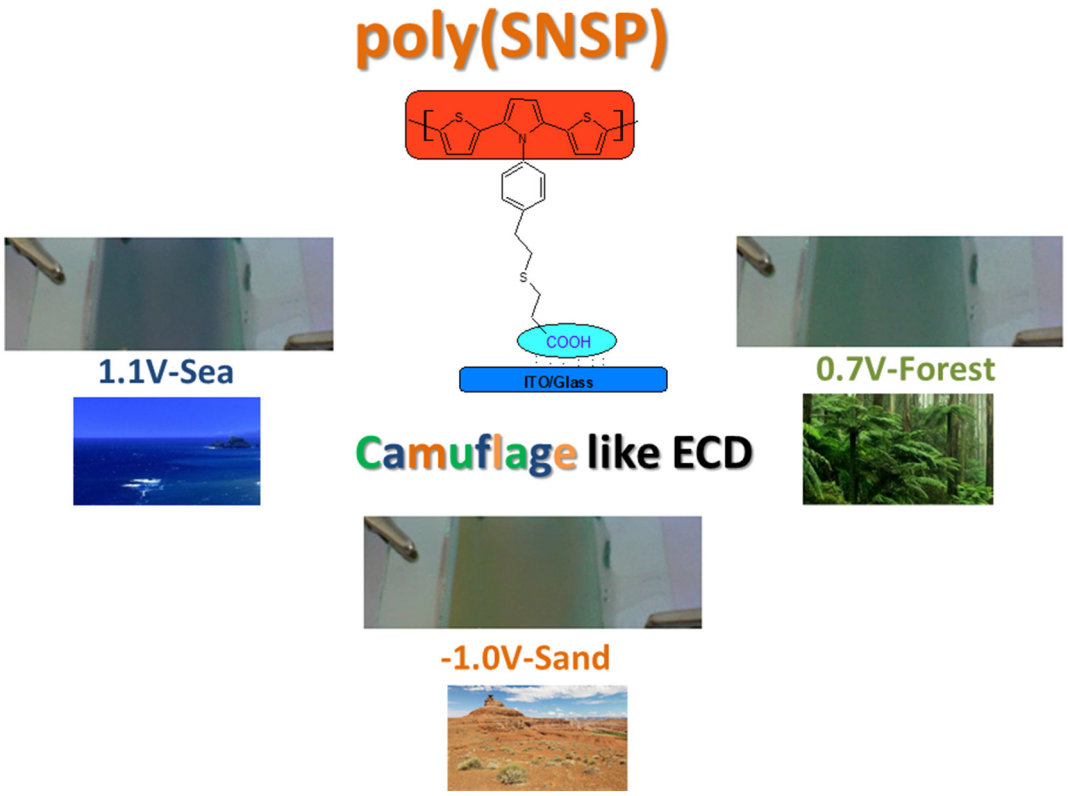

Fig. 1. Camouflage like **poly(SNSPA)**-PEDOT:PSS based complementary ECD.

electrochemical measurements revealed multielectrochromic behavior during the electrochemical oxidation process. Further, the prepared **poly(SNSPA)**-PEDOT:PSS-based complementary ECD presented low response time and high contrast ratio in the visible region, with reversible color change among soil-like brown, vegetation-like green, and sea-like blue. Because of this property, the device has multiple camouflage abilities, thus making it suitable for sand, forest, and sea surface conditions [31, 32] (Fig. 1).

2. Experimental

2.1. Materials and instrumentation

All chemicals were purchased from Aldrich and TCI Chemical, and they were used without further purification. The syntheses and characterizations of 1,4-bis(2-tiyenil)butan-1,4-dione (1) were previously described in the literature [23]. Finaly, the SNSPA was synthesized in three steps (Scheme 1).

Fourier-transform infrared spectra (FT-IR) were recorded on a Agilent Cary 630 FT-IR by using an attenuated total reflectance (ATR) module (4000–650 cm^{-1}). ^{1}H NMR spectrum was recorded on a Bruker Advance DPX-400 at 25 °C in d-$CHCl_3$ solutions. A biologic SP50 potentiostat–galvanostat system was used in the electrochemical measurements. The electrochemical cell consisted of a Ag wire as the reference electrode, a Pt wire as the counter electrode, and glassy carbon as the working electrode (WE) immersed in 0.1 M tetrabutylammonium hexafluorophosphate ($TBAPF_6$) as the supporting electrolyte.

The electrochemical measurements were realized under argon atmosphere. Further, the oxidation and reduction onset potentials determined by cyclic voltammetry (CV) were used for the HOMO-LUMO band gap calculations by using the equation $E_{HOMO} = -e(E_{ox} - E_{Fc}) + (-4.8\,eV)$, with the ferrocene redox couple $E(Fc/Fc^{+}) = 0.44$ V as the inner standard [33]. On the other hand, the optical band gaps (E_g) of **SNSPA** and the corresponding polymer were calculated by using their absorption edges of the UV–Vis spectra recorded using an Analytic Jena Speecord S-600 diode-array spectrophotometer [34]. PTI QM1 fluorescence spectrophotometer was used in the photoluminescence measurements, and all the measurements were made at a concentration of 3×10^{-5} M THF solution at 25 °C.

A Nanosurf Naio atomic force microscope (AFM) was used for the investigation of SNSPA polymer film surface. AFM measurements were made in noncontact mode (wave mode) at ambient conditions and room temperature scanned in a 10 μm × 10 μm measurement area. The AFM system was protected with an acoustic chamber to avoid electromagnetic noise.

Spectro-electrochemical measurements of SNSPA polymer film were made from absorption spectra obtained by applying a potential to this polymer film on the ITO/glass conducting surface [35]. These measurements were carried out in a spectro-electrochemical cell including a quartz cuvette, an Ag wire as the reference, and a Pt wire as the counter electrode in 0.1 M $TBAPF_6$ supporting electrolyte in acetonitrile. Colorimetry measurements were made by using a chromameter module (standard illuminator D65, field of view 10° observer) on an Analytic Jena Specord S600 UV–vis spectrophotometer with viewing geometry as recommended by International Commision on Illumination (CIE).-Color can be described in terms of three characteristics: luminance (L), hue (a), and saturation (b), according to the CIE system [36]. These values were given in the neutral, intermediate, and fully oxidized states of the **SNSPA** polymer film on the ITO/glass surface and its ECDs.

2.2. Synthesis of 1-(4-ethenylphenyl)-2,5-di(thiophen-2-yl)-1H-pyrrole (SNSP)

1,4-Dithiophene-2-yl-butane-1,4-dione (1.5 g, 6 mmol), 4-vinylaniline (0.783 g, 6,6 mmol), and p-toluenesulfonic acid (20.4 mg, 1.2 mmol) in 60 mL dry toluene were added in a flask under argon atmosphere. The reaction mixture was refluxed for 5 h by using a Dean–Stark apparatus until all the starting materials were consumed. It was then cooled, and toluene as a solvent was removed by a rotary evaporator. The residue was purified by column chromatography

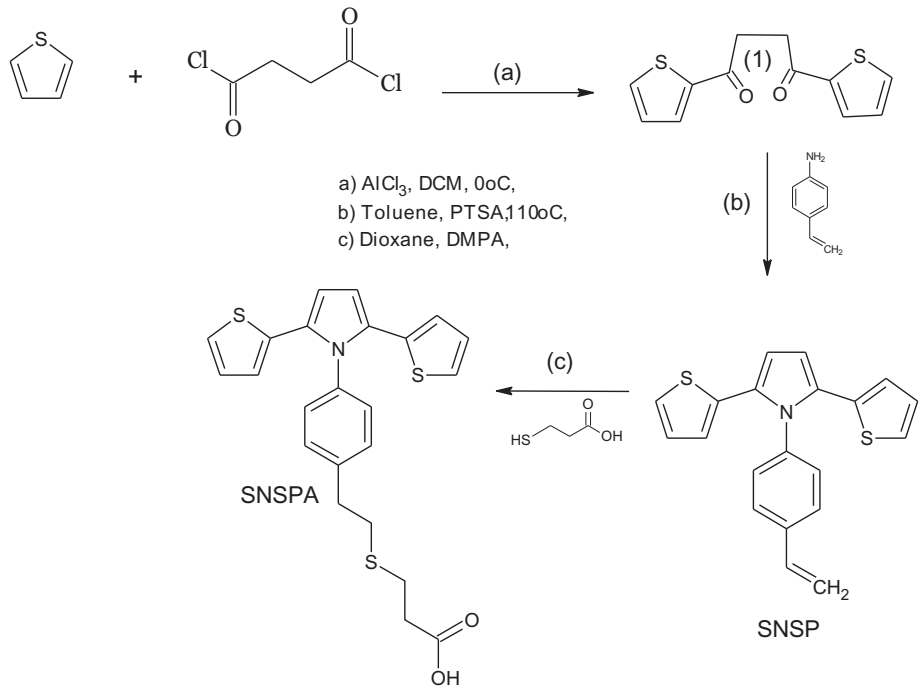

Scheme 1. Synthetic route to **SNSPA** electroactive monomer.

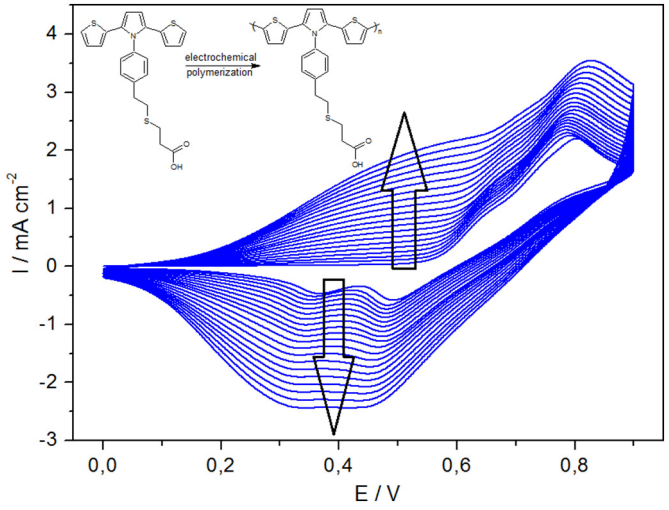

Fig. 2. Repeated potential scans of **SNSPA** in 0.1 M $TBAHF_6$ in acetonitrile, scan rate 100 mV/s.

through silica gel by eluting with a chloroform: hexane(1:2) mixture. Yield: 0.846 g, 42%, light yellow product.

FT-IR (cm^{-1}): 3104, 3068 (C—H aromatic); 3024 (C—H vinyl); 1508, 1482 (C=C aromatic); 652 (C—S thiophene); ^{1}H NMR ($CHCl_3$-d): δ ppm, 8.12 (d, 2H, Ar-H_a); 8.08 (t, 2H, Ar-H_b); 7.81 (d, 2H, Ar-H_c); 7.11 (d, 2H, Ar—H_f), 7.08 (d, 2H, Ar—H_e); 6.26 (s, 2H, Ar-H_d); 6,11, 5.52, 5.25(m, 3H, C—H vinyl subunit). *^{13}C NMR ($CHCl_3$-d): δ ppm 144.2, 136.8, 134.7, 134.2, 130.6, 128.7, 123.4, 121.6, 118.8, 117.6, 109.1, 106.8.*

2.3. Synthesis of 3-(2-[4-(2,5-di-2-thienyl-1H-pyrrol-1-yl)phenyl]ethyl-thio)propanoic acid (SNSPA)

SNSP was functionalized according to the procedures published by Cakir et al. for thiol-ene click reaction [37]. **SNSP** (0.667 g, 2 mmol),-mercaptopropionic acid (0.53 g, 5 mmol) and 1,4 dioxane (10 mL) were added to a Schlenk tube. The reaction mixture was degassed by argon under vacuum. DMPA (0.01 g, 0.04 mmol) was then added, and the reaction mixture was stirred at room temperature under 366 nm UV light for an hour. The mixture was poured into 100 mL of methanol, and the solvent was removed under reduced pressure. The residue was purified by column chromatography through silica gel by eluting with a chloroform: methanol (9:1) mixture. Yield: 0.622 g, 70%, gray product.

FT-IR (cm^{-1}): 3096, 3061 (C—H aromatic); 2917, 2847 (C—H aliphatic); 1707(C=O carboxyl); 1586, 1488 (C=C aromatic); 684 (C—S thiophene); ^{1}*H NMR ($CHCl_3$-d): δ ppm, 8.16 (d, 2H, Ar-H_a); 8.13 (t, 2H, Ar-H_b); 7.87 (d, 2H, Ar-H_c); 6.92 (d, 2H, Ar—H_e); 6.90 (d, 2H, Ar—H_f), 6.26 (s, 2H, Ar-H_d); 3.86 (d, 2H, H_j); 3.57 (d, 2H, H_i); 3.31 (d, 2H, H_h), 2.72 (d, 2H, H_g);* ^{13}*C NMR ($CHCl_3$-d): δ ppm 179.2 (COOH), 143.4, 135.6, 134.1, 132.8, 130.9, 128.3, 121.8, 119.3, 118.4, 109.1, 36.8, 34.7, 31.6, 27.3.*

2.4. Electrochemical polymerization of SNSPA

Repeated scan electrochemical polymerization was carried out by using an acetonitrile solution of 2.0×10^{-3} M **SNSPA** monomer and 0.1 M $TBAPF_6$. In addition, a platinum wire was used as the counter and Ag wire as the reference electrode. **Poly(SNSPA)** film was obtained by performing repetitive cycling for 20 times at potentials between 0 and 0.9 V and a scan rate of 100 mV/s (Fig. 2). A new redox couple with a half wave potential ($E_{m,\ 1/2}^{ox}$) of 0.48 V was observed, and the reversible peaks intensified after each successive cycle, which clearly indicates the deposition of **poly(SNSPA)** on the ITO-glass working electrode surface. The prepared polymer film was then rinsed with acetonitrile to remove electrolyte salt and other impurities. Thus, the SNSPA polymer film could be directly formed on the ITO-glass surface (8–12 Ω, 0.8 cm × 5 cm and 4 cm × 5 cm).

2.5. ECD fabrication

The ECD was fabricated in a sandwich configuration by using a transparent ITO-glass substrate (active area: 5 cm^2) as anode and cathode materials. First, PEDOT–PSS was spin coated from aqueous solution (Clevios pH 500 - Heraeus) onto the ITO-glass surface (5 cm^2)

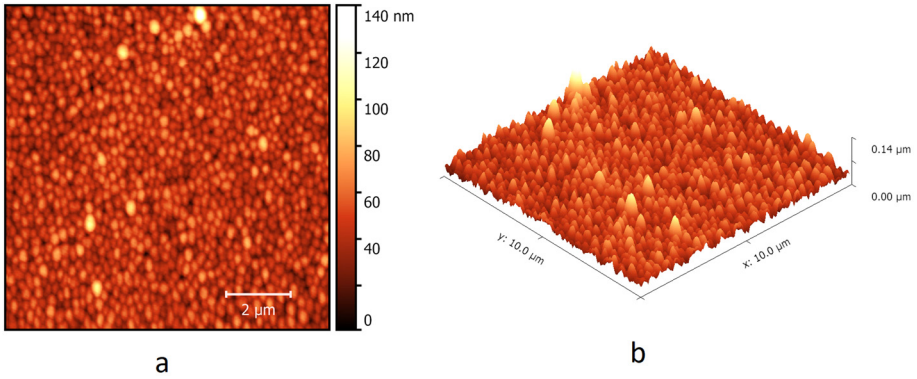

Fig. 3. AFM image of poly(SNSPA) thin film surface; a) Topography image b) 3D image.

with 2000 rpm spin rate. On the other hand, **poly(SNSPA)** was deposited onto another ITO-glass surface by potentiodynamic electrochemical process. After the process, the polymer film of **poly(SNSPA)** was rinsed with acetonitrile to remove electrolyte salt. The conducting gel electrolyte was prepared from $LiClO_4$:ACN:poly (methyl methacrylate) (PMMA, Mw: 15,000):1,2-propylene carbonate in the ratio of 3:70:7:20 by weight. Finally, the gel electrolyte was spread over each face, and individual ITO/glass layers were stacked face to face [38, 39].

3. Results and discussion

3.1. Thin film properties

The surface morphology of **poly(SNSPA)** film obtained by the electrochemical deposition process was examined by AFM (Fig. 3). As provided in the literature, during electrochromic switching, the electrolyte ions are injected/ejected upon the polymer film formed on the ITO-glass WE surface [40, 41]. Because of this feature, the electrochromic performance can be affected by the polymer film surface roughness [42–44]. The AFM image of **poly(SNSPA)** exhibits a uniform structure because the polymer could be regularly attached to the ITO-glass surface through a compatible –COOH subunit. Overall, the root mean surface roughness of the polymer was found to be 0.4 nm with 234 nm polymer film thickness. Consequently, a well-defined thin film surface and uniform roughness are great advantages for electrochromic applications.

3.2. Electrochemical properties

The electrochemical properties of **SNSPA** monomer and the corresponding polymer were investigated by CV (Fig. 4). During the cathodic scan regime, a semi-reversible reduction peak attributed to carboxyl subunit at $E_{m,\ a}^{red} = -1.45$, $E_{m,\ c}^{red} = -1.51$ V, and $E_{m,\ 1/2}^{ox} = -1.48$ V was observed in the CV of **SNSPA** monomer. This reduction peak negatively shifted to $E_{p,\ a}^{red} = -1.70$, $E_{p,\ c}^{red} = -1.76$ V, and $E_{p,\ 1/2}^{ox} = -1.73$ V in **poly(SNSPA).** On the other hand, a reversible oxidation peak was defined at $E_{m,\ a}^{ox} = 0.79$ V, $E_{m,\ c}^{ox} = 0.63$ V, and $E_{m,\ 1/2}^{ox} = 0.71$ V for **SNSPA**, and because of extended conjugation after polymerization, the oxidation was observed at lower potentials; $E_{p,\ a}^{ox} = 0.71$ V, $E_{p,\ c}^{ox} = 0.51$ V, and $E_{p,\ 1/2}^{ox} = 0.61$ V for **poly(SNSPA)** in the anodic regime. Furthermore, the electrochemical band gaps of **SNSPA** and corresponding polymer were calculated by using onset values of their redox potentials (Table 1).

3.3. Optical properties

The optical properties of **SNSPA** were investigated by bot UV–vis absorption and fluorescence spectroscopy recorded with a concentration of 2×10^{-6} M solution in THF (Fig. 5). On the other hand, the **poly(SNSPA)** film on ITO/glass surface was rinsed in THF to obtain the **SNSPA** polymer solution. **SNSPA** exhibited three distinct absorption bands at 232, 268 and 337 nm. The transition at 337 nm is more intense than that at the neighboring band at 268 nm because **SNSPA** bears both SNS-conjugated system containing thiophene and pyrrole photoactive moieties and –COOH as subunit. In the UV–vis absorption spectrum of **poly(SNSPA)**, a 185 nm red shift was observed after polymerization because of the extended conjugation on the electroactive **SNSPA** polymer main chain. Finally, the optical band gap (E_g) of **SNSPA** and **poly(SNSPA)** calculated from their absorption edges were found to be 2.11 eV and 1.90 eV, respectively (Table 1). Photoluminescence behavior of **SNSPA** and **poly(SNSPA)** were also investigated in the same conditions with exciting their low-energy absorption maxima. In the photoluminescence spectrum of SNSPA, two distinct emission bands were observed at 378 and 422 nm. Besides, the spectrum of **poly (SNSPA)** exhibited emission maxima at 628 nm relative to the corresponding monomer **SNSPA** because of a red shift in absorbance. Finally, it is clearly observed that blue light emission of the **SNSPA** solution in THF turned into green after polymerization (Fig. 5) (Table 2).

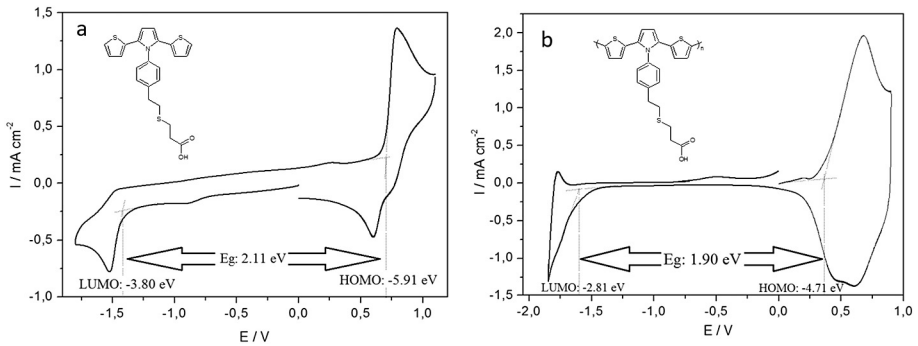

Fig. 4. Redox behavior of **SNSPA (a)** and **poly(SNSPA) (b)** in 0.1 M $TBAPF_6$/acetonitrile electrolyte solution at a scan rate of 100 mV/s, vs. Ag wire.

Table 1
HOMO and LUMO energy levels, electrochemical ($E_g^{'}$) and optical band gap (E_g) values of **SNSPA** and **poly(SNSPA)**.

Molecule	HOMO (eV)	LUMO (eV)	Optical band gap (eV)	Electrochemical band gap (eV)
SNSPA	−5.91	−3.80	3.18	2.11
Poly(SNSPA)	−4.71	−2.81	2.13	1.90

3.4. Spectroelectrochemical properties

The electrochromic behavior of the **poly(SNSPA)** film on the ITO-glass surface was investigated by spectro-electrochemical technique. At the neutral state, the **poly(SNSPA)** film is in orange color, which absorbs the blue-green region on the visible spectrum. Depending on the applied positive potential, while the intensity of the absorption band at about 430 nm was decreased, the absorption band around 650 nm gradually intensified between 0 and 0.6 V. As a result, the orange color of the **poly(SNSPA)** film (L*:93.49; a:-1.30; b: 54.44) was turned into green (L*:73.38; a:-13.29; b: 4.23) at the intermediate state. With further increase in the potential from 0.6 to 1.1 V, the band at 860 nm was intensified, and the green color of the polymer film converted to dark blue (L*:62.74; a:-0.88; b:-21,63) at fully oxidized state (Fig. 6). This multielectrochromic behavior has great advantage in potential applications.

On the other hand, the ECD was prepared in sandwich configuration by ITO-glass/PEDOT:PSS//$LiClO_4$ gel electrolyte//poly(SNSPA)/ITO-glass device construction. PEDOT:PSS and **poly(SNSPA)** layers were prepared by spin coating and electrochemical deposition process, respectively. Then, in the second step, an $LiClO_4$-based gel electrolyte was spread over the face of each layer. Finally, electroactive material-coated ITO-glass layers were stacked face to face. Spectroelectrochemical behavior of ECD under an applied potential of −1.0–1.2 is presented in Fig. 7. During the coloration process of dual-type ECD, **poly(SNSPA)** and PEDOT:PSS layers were oxidized and reduced, respectively. At the neutral state, **poly(SNSPA)** layer was orange and PEDOT:PSS layer was light blue; therefore, the color of the ECD was light brown (L*:70.21; a: 4.35; b: 15.98). When a potential of −1.0 to 0.7 V was applied, the new band at about 740 nm was intensified; hence, the light brown color of ECD turned into green (L*:67.79; a: −1.54; b: 2.53) at the intermediate state. At higher potentials from 0.7 to 1.2 V, the new band at about 540 nm was intensified because of the simultaneous oxidation of poly (SNPA) and reduction of PEDOT:PSS. As the spectral signatures of PEDOT:PSS layers became dominant at the fully oxidized state, the color of ECD converted to dark blue (L*:64.73; a: 2.92; b:-2.29) (Fig. 8).

The kinetic studies of **SNSPA** polymer film and the ECD were carried out by detecting the changes in the electro-optical responses during redox potential switching. **Poly(SNSPA)** film was investigated by alterations that occurred in the transmittance (increments of the absorption band at 860 nm with respect to time), while switching the potential step wisely between neutral (0 V) and oxidized states (1.1 V) with a residence time of 5 s. Response time to color change and the percentage transmittance change (ΔT%) of the polymer film during the potential switching were determined (Fig. 7). The ΔT% of **poly(SNSPA)** at 860 nm between neutral (at 0 V) and oxidized states (at 1.1 V) was detected as 56%. In addition, the oxidation and reduction response times were measured as 1.7 and 1.2 s, respectively. In addition, optical activity against applied potentials and their related life time are very important parameters for electrochromic applications. It was determined that **poly-(SNSPA)** showed an optical activity of about 97% at the end of 1000 potential switching cycles between 0 and 1.1 V. On the other hand, ΔT% of **poly(SNSPA)-PEDOT:PSS**-based ECD at 600 nm was 54% between −1.0 and 1.2 V. The response time against transmittance changes in this regime was measured as 0.65 and 0.45 s.

Table 2
Electrochromic parameters for **poly-(SNSPA)** and prepared ECD.

Material	Optical contrast change (ΔT%)	Response time (s)	Optical activity after 5000 cycles (%)	Coloration efficiency, ($cm^2\ C^{-1}$)
poly(SNSPA) *Thin film*	%ΔT: 56%$T_{neutral}$: 98%$T_{oxidation}$: 42 *at 860 nm*	Oxidation 1.7 s Reduction 1.2 s	97	82
poly(SNSPA)-PEDOT:PSS *ECD*	%ΔT: 54%$T_{neutral}$: 98%$T_{oxidation}$: 44 *at 600 nm*	Oxidation 0.65 s Reduction 0.45 s	98	434

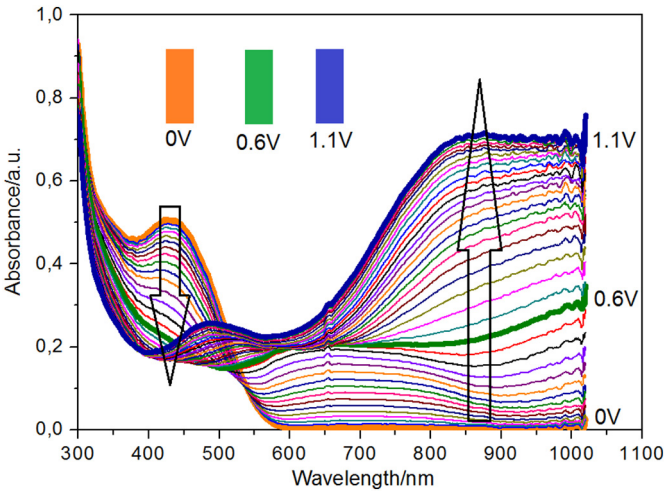

Fig. 6. Electronic absorption spectra and the color change of **poly(SNSPA)** in the anodic regime on ITO/glass surface in 0.1 M $TBAPF_6$/acetonitrile.

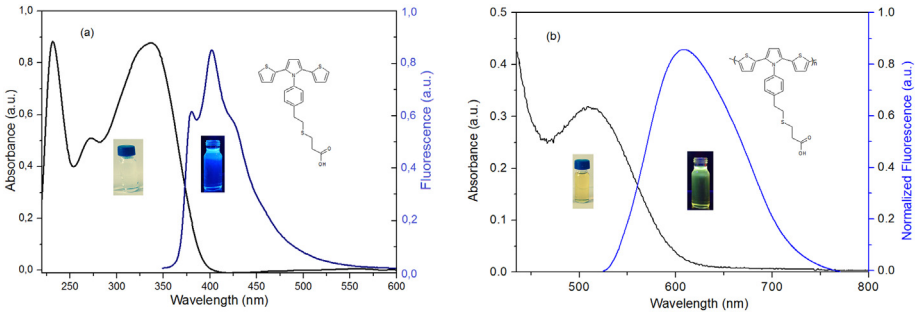

Fig. 5. UV–Vis absorption and fluorescence spectra of **SNSPA (a)** and **poly(SNSPA) (b)** in THF.

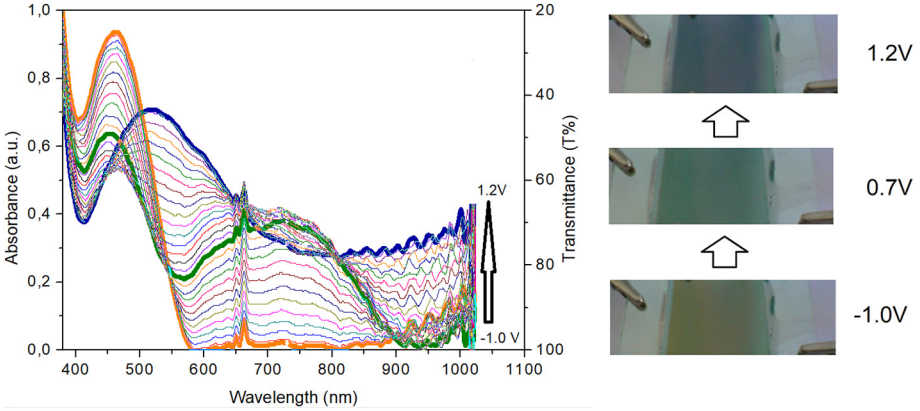

Fig. 7. Electronic absorption spectra and the color change of **poly(SNSPA)-PEDOT:PSS**-based ECD scanning potentials between −1.0 and 1.2 V.

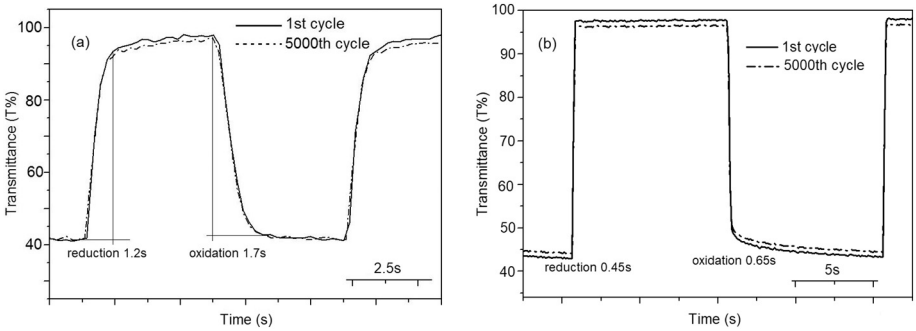

Fig. 8. Electrochromic switching and optical absorbance monitored (a) at 860 nm for **poly(SNSPA)** between 0 V and 1.1 V (b) at 600 nm for **poly(SNSPA):PEDOT:PSS**-based ECD.

Further, the ECD achieved an excellent optical activity of 98% after 5000 cycles with a residence time of 5 s (Fig. 8). The high stability and fast response time of ECD against electrochromic switching are great advantages for its use in electrochromic applications.

The CE is also important for electrochromic application. The CE was calculated as follows: CE = $\Delta OD/Q_d$ and $\Delta OD = \log (T_{colored}/T_{bleached})$, where Q_d is the injected/ejected charge between neutral and oxidized states and $T_{colored}$ and $T_{bleached}$ are the transmittance in the oxidized and neutral states, respectively [38]. By using these equations, the CEs were calculated as 82 and 434 $cm^2\ C^{-1}$ during the color switching of **SNSPA** polymer film (active area of 1 cm^2) and ECD (active area of 5 cm^2), respectively.

4. Conclusion

In this work, a new SNS-based electroactive molecule bearing –COOH subunit compatible with a ITO-glass surface was synthesized and then directly coated onto the ITO-glass surface by potentiodynamic electrochemical process. Multielectrochromic behavior among orange, green, and dark blue colors was observed in the spectro-electrochemical measurement of **poly(SNSPA)** thin film by applying a positive potential. Further, a well-ordered thin film morphology was observed in the AFM measurements of **poly(SNSPA)** film owing to the presence of ITO-compatible –COOH subunit. On the other hand, the electrochromic performance of ECDs constructed with a sandwich structure of ITO-glass/**poly(SNSPA)**//gel electrolyte//**PEDOT:PSS**/ITO-glass was investigated. The light brown color ECD at the neutral state converted to green and dark blue on scanning the potential between −1.0 and 1.2 V. In conclusion, the capability of the proposed monomer to undergo reversible color change among brown, green, and blue is crucial for use as an adaptive camouflage for all natural conditions such as sand, forest, and sea for military applications.

Acknowledgment

The authors would like to thank Çanakkale Onsekiz Mart University for financial support (Project Number: 2016/1083).

References

[1] A.G. MacDiarmid, A.J. Heeger, Organic metals and semiconductors - Polyacetylene, (Ch)X, and its derivatives, J. Electrochem. Soc. 127 (3) (1980) C83.
[2] C.W. Tang, S.A. Vanslyke, C.H. Chen, Electroluminescence of doped organic thin-films, J. Appl. Phys. 65 (9) (1989) 3610–3616.
[3] M.J. Cohen, Use of conducting polymers in low-cost solar-cells, J. Electrochem. Soc. 127 (3) (1980) C83.
[4] J.J.R. Arias, M.D.V. Marques, Performance of poly(3-hexylthiophene) in bulk heterojunction solar cells: influence of polymer size and size distribution, React. Funct. Polym. 113 (2017) 58–69.
[5] J. Paloheimo, P. Kuivalainen, H. Stubb, E. Vuorimaa, P. Ylilahti, Molecular field-effect transistors using conducting polymer Langmuir-Blodgett-films, Appl. Phys. Lett. 56 (12) (1990) 1157–1159.
[6] M.S. Lu, H.C. Wu, Y.W. Lin, M. Ueda, W.C. Chen, Low voltage operation of non-volatile flexible OFET memory devices using high-k P(VDF-TrFE) gate dielectric and polyimide charge storage layer, React. Funct. Polym. 108 (2016) 39–46.
[7] F. Garnier, G. Tourillon, M. Gazard, J.C. Dubois, Organic conducting polymers derived from substituted Thiophenes as electrochromic material, J. Electroanal. Chem. 148 (2) (1983) 299–303.
[8] S.H. Hsiao, Y.H. Hsiao, Y.R. Kung, C.M. Leu, T.M. Lee, Triphenylamine-based redox-active aramids with 1-piperidinyl substituent as an auxiliary donor: enhanced electrochemical stability and electrochromic performance, React. Funct. Polym. 108 (2016) 54–62.
[9] C. Taliani, G. Ruani, R. Zamboni, A. Bolognesi, M. Catellani, S. Destri, W. Porzio, P. Ostoja, Optical-properties of a low-energy gap conducting polymer - Polydithieno [3,4-B-3′,4′-D]Thiophene, Synthetic Met 28 (1–2) (1989) C507–C514.
[10] B. Kiskan, Adapting benzoxazine chemistry for unconventional applications, React. Funct. Polym. 129 (2018) 76–88.
[11] G.A. Sotzing, J.R. Reynolds, P.J. Steel, Electrochromic conducting polymers via electrochemical polymerization of bis(2-(3,4-ethylenedioxy)thienyl) monomers, Chem. Mater. 8 (4) (1996) 882–889.
[12] J.P. Randin, Ion-containing polymers as semisolid electrolytes in Wo3-based electrochromic devices, J. Electrochem. Soc. 129 (6) (1982) 1215–1220.
[13] S.F. Cogan, T.D. Plante, R.S. Mcfadden, R.D. Rauh, Solar modulation in a-Wo3 a-Iro2 and C-Kxwo3 + (X/2) a-Iro2 complementary electrochromic windows, Sol

Energ Mater 16 (5) (1987) 371–382.
[14] P.M. Beaujuge, J.R. Reynolds, Color control in pi-conjugated organic polymers for use in electrochromic devices, Chem. Rev. 110 (1) (2010) 268–320.
[15] C.L. Tsai, H.J. Yen, G.S. Liou, Highly transparent polyimide hybrids for optoelectronic applications, React. Funct. Polym. 108 (2016) 2–30.
[16] H.F. Wang, M. Barrett, B. Duane, J. Gu, F. Zenhausern, Materials and processing of polymer-based electrochromic devices, Mater Sci Eng B-Adv 228 (2018) 167–174.
[17] R.J. Mortimer, Electrochromic materials, Chem. Soc. Rev. 26 (3) (1997) 147–156.
[18] J. Jensen, M.V. Madsen, F.C. Krebs, Photochemical stability of electrochromic polymers and devices, J. Mater. Chem. C 1 (32) (2013) 4826–4835.
[19] K.R. Lee, G.A. Sotzing, Green and blue electrochromic polymers from Processable siloxane precursors, Chem. Mater. 25 (14) (2013) 2898–2904.
[20] S. Suganya, N. Kim, J.Y. Jeong, J.S. Park, Benzotriazole-based donor-acceptor type low band gap polymers with a siloxane-terminated side-chain for electrochromic applications, Polymer 116 (2017) 226–232.
[21] L. Beverina, G.A. Pagani, M. Sassi, Multichromophoric electrochromic polymers: colour tuning of conjugated polymers through the side chain functionalization approach, Chem. Commun. 50 (41) (2014) 5413–5430.
[22] K.S. Ryder, L.F. Schweiger, A. Glidle, J.M. Cooper, Strategies towards functionalised electronically conducting organic copolymers: part 2, Copolymerisation, J Mater Chem 10 (8) (2000) 1785–1793.
[23] L.F. Schweiger, K.S. Ryder, D.G. Morris, A. Glidle, J.M. Cooper, Strategies towards functionalised electronically conducting organic copolymers, J. Mater. Chem. 10 (1) (2000) 107–114.
[24] S. Varis, M. Ak, C. Tanyeli, I.M. Akhmedov, L. Toppare, Synthesis and characterization of a new soluble conducting polymer and its electrochromic device, Solid State Sci. 8 (12) (2006) 1477–1483.
[25] A. Cihaner, F. Algi, An electrochromic and fluorescent polymer based on 1-(1-naphthyl)-2,5-di-2-thienyl-1H-pyrrole, J. Electroanal. Chem. 614 (1–2) (2008) 101–106.
[26] S. Koyuncu, C. Zafer, E. Sefer, F.B. Koyuncu, S. Demic, I. Kaya, E. Ozdemir, S. Icli, A new conducting polymer of 2,5-bis(2-thienyl)-1H-(pyrrole) (SNS) containing carbazole subunit: electrochemical, optical and electrochromic properties, Synthetic Met 159 (19–20) (2009) 2013–2021.
[27] E. Sefer, H. Bilgili, B. Gultekin, M. Tonga, S. Koyuncu, A narrow range multi-electrochromism from 2,5-di-(2-thienyl)-1H-pyrrole polymer bearing pendant perylenediimide moiety, Dyes Pigments 113 (2015) 121–128.
[28] E. Sefer, F.B. Koyuncu, E. Oguzhan, S. Koyuncu, A new near-infrared switchable electrochromic polymer and its device application, J Polym Sci Pol Chem 48 (20) (2010) 4419–4427.
[29] A. Cihaner, F. Algi, A new conducting polymer bearing 4,4-difluoro-4-bora-3a,4a-diaza-s-indacene (BODIPY) subunit: synthesis and characterization, Electrochim. Acta 54 (2) (2008) 786–792.
[30] A. Cihaner, F. Algi, A processable rainbow mimic fluorescent polymer and its unprecedented coloration efficiency in electrochromic device, Electrochim. Acta 53 (5) (2008) 2574–2578.
[31] H.T. Yu, S. Shao, L.J. Yan, H. Meng, Y.W. He, C. Yao, P.P. Xu, X.T. Zhang, W.P. Hu, W. Huang, Side-chain engineering of green color electrochromic polymer materials: toward adaptive camouflage application, J. Mater. Chem. C 4 (12) (2016) 2269–2273.
[32] S. Beaupre, A.C. Breton, J. Dumas, M. Leclerc, Multicolored electrochromic cells based on poly(2,7-Carbazole) derivatives for adaptive camouflage, Chem. Mater. 21 (8) (2009) 1504–1513.
[33] J. Heinze, B.A. Frontana-Uribe, S. Ludwigs, Electrochemistry of conducting polymers-persistent models and new concepts, Chem. Rev. 110 (8) (2010) 4724–4771.
[34] A.O. Patil, A.J. Heeger, F. Wudl, Optical-properties of conducting polymers, Chem. Rev. 88 (1) (1988) 183–200.
[35] W. Kaim, J. Fiedler, Spectroelectrochemistry: the best of two worlds, Chem. Soc. Rev. 38 (12) (2009) 3373–3382.
[36] R.J. Mortimer, J.R. Reynolds, In situ colorimetric and composite coloration efficiency measurements for electrochromic Prussian blue, J. Mater. Chem. 15 (22) (2005) 2226–2233.
[37] N. Cakir, U. Tunca, G. Hizal, H. Durmaz, Heterofunctionalized multiarm star polymers via sequential thiol-Para-Fluoro and thiol-Ene double "click" reactions, Macromol Chem Physic 217 (5) (2016) 636–645.
[38] G. Sonmez, H. Meng, F. Wudl, Organic polymeric electrochromic devices: Polychromism with very high coloration efficiency, Chem. Mater. 16 (4) (2004) 574–580.
[39] M. Sezgin, O. Ozay, S. Koyuncu, H. Ozay, F.B. Koyuncu, A neutral state colorless phosphazene/carbazole hybride dendron and its electrochromic device application, Chem. Eng. J. 274 (2015) 282–289.
[40] Q. Zhang, C.Y. Tsai, T. Abidin, J.C. Jiang, W.R. Shie, L.J. Li, D.J. Liaw, Transmissive-to-black fast electrochromic switching from a long conjugated pendant group and a highly dispersed polymer/SWNT, Polym Chem-Uk 9 (5) (2018) 619–626.
[41] S.H. Hsiao, G.S. Liou, Y.C. Kung, H.J. Yen, High contrast ratio and rapid switching electrochromic polymeric films based on 4-(dimethylamino)triphenylamine-functionalized aromatic polyamides, Macromolecules 41 (8) (2008) 2800–2808.
[42] P.P. Xu, I. Murtaza, J.J. Shi, M.M. Zhu, Y.W. He, H.T. Yu, O. Goto, H. Meng, Highly transmissive blue electrochromic polymers based on thieno[3,2-b]thiophene, Polym Chem-Uk 7 (34) (2016) 5351–5356.
[43] Y. Xiao, G.B. Dong, J.J. Guo, Q.R. Liu, Q.J. Huang, Q.Q. Zhang, X.L. Zhong, X.G. Diao, Thickness dependent surface roughness of sputtered Li2.5TaOx ion conductor and its effect on electro-optical performance of inorganic monolithic electrochromic device, Sol Energ Mat Sol C 179 (2018) 319–327.
[44] G. Tahtali, Z. Has, C. Doyranli, C. Varlikli, S. Koyuncu, Solution processable neutral state colourless electrochromic devices: effect of the layer thickness on the electrochromic performance, J. Mater. Chem. C 4 (42) (2016) 10090–10094.